View metadata, citation and similar papers at core.ac.uk

brought to you by CORE

provided by NASA Technical Reports Server

N85-22505

CHARACTERISTICS OF EMI GENERATED BY NEGATIVE METAL/POSITIVE DIELECTRIC VOLTAGE STRESSES DUE TO SPACECRAFT CHARGING

R. C. Chaky and G. T. Inouye
TRW Space and Technology Group
Redondo Beach, California 90278

Charging of spacecraft surfaces by the environmental plasma can result in differential potentials between metallic structure and adjacent dielectric surfaces in which the relative polarity of the voltage stress is either negative dielectric/positive metal or negative metal/positive dielectric. The first stress polarity, negative dielectric/positive metal, has been studied extensively in prior work in which dielectric targets were bombarded with electrons. The second polarity, negative metal/positive dielectric, has not had much research attention, although this stress condition may arise if relatively large areas of spacecraft surface metals are shadowed from solar UV and/or if the UV intensity is reduced as in the situation in which the spacecraft is entering into or leaving eclipse. In this paper we present results of experimental studies of negative metal/positive dielectric systems.

NASCAP charging analyses and SCATHA data have shown that differential stresses greater than 3-6 kV of either polarity are not easily generated on spacecraft exposed to the geosynchronous orbit environment. Measurements by many workers have shown that negative dielectric/positive metal electrostatic discharge (ESD) thresholds are in the 10-20 kV range. Negative metal/positive dielectric discharge thresholds are in the 1-3 kV range, and are therefore much more likely to be the source of in-orbit electromagnetic interference (EMI). Prior studies (1, 2, 3) have identified this more viable arc discharge mode in a qualitative sense. Figure 1 illustrates some of the features of the phenomena associated with the negative metal/positive dielectric configuration. Figure 1 is a strip chart record obtained with a solar cell test sample biased negatively by a power supply through a 10 kilomegohm series resistor. The positive dielectric (cover glass) potential is generated by photoemission induced by UV irradiation. The setup is shown in Figure 2. The voltage-divided substrate voltage, V, provides the input for the strip chart recorder. With the bias voltage applied, turning on the UV reduces the substrate voltage by the normal photoemission current IR drop, i.e., the sample voltage V_s drops from 7.1 kilovolts to 6.9 kilovolts. Shortly after the lamps are turned on arc discharges, blowoff of electrons, are seen as momentary pulses raising the substrate voltage towards zero volts. About a minute later the substrate voltage settles below -1 kV, a steady-state condition of enhanced electron emission. The noisiness of the enhanced emission current should be noted. At 7.32 minutes the UV lamps are turned off, but the enhanced electron emission (e^3) continues. This condition may

PRECEDING PAGE BLANK NOT FILMED

continue for tens of minutes or may abruptly or gradually "wear out" and return to a normal photoemission level with the UV lamps on, and only arc discharge, or may revert to the e^3 state. The phenomena associated with the negative metal/positive dielectric configuration are summarized below:

- o Arc discharges at low voltages (1-3 kV)
- o Enchanced electron emission (e^3)
- o Corona-like noise associated with e^3

Figure 3 shows the surface and structure potentials relative to the far plasma calculated as a function of the solar UV intensity for a three-axis stabilized spacecraft. In full sunlight, sunlit dielectric surfaces as well as structure are a few volts positive, mainly because of the predominance of photoemission currents over the incident negative currents due to the substorm electrons. Dark dielectric surfaces, surfaces shadowed by other parts of the spacecraft, are 2-3 kV negative because these surfaces are not photoemitting. As the UV intensity is decreased, the structure potential drops towards -3 kV first because its exposed surfaces are both sunlit and shadowed. The sunlit dielectric surfaces eventually also drop to -3 kV at about 20% of full sunlight. At zero UV intensity, complete eclipse, all potentials are nearly equal at about -3 kV.

Figure 4 shows the differential voltages relative to structure computed from the data for Figure 3. The positive dielectric voltages, the sunlit surfaces, peak at about plus 2.8 kV at about 20% of full sunlight, a photoemission current density, J_{uv}, of above 0.5 na/cm^2. This, then, is the regime in which the low voltage reversed polarity arc discharges may be expected to occur most readily. Figure 5, from the paper by H. C. Koons (4), shows arc discharges observed on the P78-2 (SCATHA) satellite as it goes into and out of eclipse during a substorm.

Arc discharge blowoff current magnitudes and those of the associated replacement currents depend on the capacitance of the spacecraft to space. This capacitance to space is directly proportional to the linear dimensions of the spacecraft, and hence the hazard due to blowoff will increase as spacecraft become larger in future designs. Structural replacement currents are collected over all spacecraft surfaces and flow back towards the arcing source. They become more and more concentrated near the source, but the possibility exists for coupling unwanted EMI into victim circuits remote from the source. The flashover component of a positive dielectric discharge increases with the source dimension, but its effects are confined to localized electrostatic and magnetic coupling. The peak voltage associated with these discharges was found to be that of the negative metal potential prior to the discharge, a positive-going step in 0.5 to 1.5 microseconds. The recovery time to re-adjust to the original negative potential was the RC recharge time constant, on the order of a fraction of a millisecond.

Another facet of the EMI generated by the negative metal/positive dielectric configuration arises if it results in the enhanced steady-state corona-like electron emission condition. The emission currents exhibit an impulsive noise characteristic which increases in amplitude and frequency of occurrence with the level of emission current. We interpret this noise

characteristic as being due to the burn-up of localized sharply pointed high field emission sources. Peak noise voltages of 1.5 kV and currents of 4 microamps have been observed on a strip chart recorder (0-10 Hz bandwidth). On a wide band oscilloscope the amplitude and risetimes may approach those of the individual discharges discussed earlier.

TEST CONFIGURATION

Test were performed in a 2' x 4' vacuum chamber at pressures between 10^{-5} and 10^{-6} Torr. Negative sample substrate potentials were obtained with a high voltage power supply, and the more positive but still negative dielectric surface potentials were obtained by irradiation with mercury UV lamps. The test setup for EMI characterization is shown in Figure 6. Earlier tests by Inouye and Sellen (1) applied the negative bias with an electron beam from a gun located at the opposite end of the vacuum chamber to more nearly simulate the in-orbit situation. The adjustable (0 to 20 kV) power supply with selectable series resistor, R_1 (80 Meg to 10 kMeg), provides a more easily controlled and defined source of negative bias.

The 25 kMeg - 1 Meg resistive divider tied to the point between R_1 and the sample performs two important functions. First, it provides a convenient measure of sample voltage, and because of the IR_1 voltage drop, the sample emission current. The strip chart record of Figure 1 was obtained at this test point. Even more important, the 25 kMeg, in parallel with R_1, isolates the sample from the vacuum system ground and allows the sample potential to more nearly simulate equilibration as it would occur in orbit. Short duration arc discharge voltage swings and associated currents will also be more closely simulated than in test configurations in which low impedance (power supply output impedances, 50 ohm cable terminations) were used.

The strip chart record provides a low frequency (0-10 Hz) measure of the sample voltage and current which is fine as an indication of equilibration currents, but is only a qualitative measure of the total electromagnetic interference (EMI) situation. The additional circuitry shown in Figure 6 provides the necessary diagnostics to define the higher frequency EMI components. The test sample is further isolated with a 15 Meg resistor, and C_1/C_2 is a capacitive voltage divider, just outside the vacuum chamber, which provides a measure of sample voltage. The 1 ohm resistor at the bottom of C_2 provides a direct measure of the sample current. C_1, 25 pf to 0.1 μf, represents the spacecraft capacitance to space. These two capacitance values, for a spherical spacecraft, represent spacecraft radii of 0.5 m and 1 km respectively, and will be demonstrated that the spacecraft dimension has a critical effect on the character of arc discharges.

The sample voltages and currents measured by C_1, C_2 and the 1 ohm resistor and the strip chart record provide a measure only of emitted or blowout currents. Another component, the flashover currents which flow from the front of the dielectric directly to the substrate, cannot be detected at the 1 ohm resistor. That this component exists and that a uniform wipeoff of the initial charge occurs has been demonstrated by scanning the dielectric surface potential with an electrostatic voltage probe (not shown in Figure 6) before and after a discharge. A loop antenna with its axis parallel to the

plane of the dielectric has been installed to attempt to obtain a measure of the flashover currents. Since the direction of surface current flow is random, only a qualitative indication is to be expected. The blowout component may also couple magnetic flux into this horizontal loop. Its time history, however, is known from the 1 ohm resistor, and therefore the loop may provide data on the flashover component.

Two stainless steel wire meshes are located in front of the test sample between the sample and the UV lamps. They have a transparency of 80 to 90 percent and hence do not materially affect the UV intensity at the sample. These meshes were installed to detect separately the electrons and the positive ion components of the blowoff current. The first grid is grounded through 50 ohms, and the second is biased negatively, after filtering, from the power supply. The first grid at ground potential is necessary to permit photoelectrons to leave the dielectric surface, thus biasing that surface positively relative to the metallic substrate.

TEST RESULTS

The majority of test samples in the tests reported here were solar cells mounted in the configuration shown in Figure 7. Table 1 lists the eight various combinations of coverglass material, interconnect type and insulation (or not) from the aluminum substrate. Samples 9 and 10 were duplicates of Sample 1 and 2. One objective of the tests was to determine which type of sample exhibited enhanced electron emission and which did not. Only a few samples exhibited e^3, and not all arc discharged. Table 2 summarizes the results.

The following results on detailed EMI characteristics were obtained on a solar cell sample with the normal interconnects, fused silica coverglass and Kapton insulation, Sample No. 1 on Table 1. Figure 8 is a plot of the steady-state e^3 current versus sample voltage. It shows that e^3 currents become significant above 200 volts and increase monotonically with increasing sample voltage. Figure 9 is a plot of peak noise currents as seen on the strip chart record (0-10 Hz) as a function of the dc e^3 current. Peak noise voltages of 1.5 kV and 4 microamperes in amplitude have been observed. On a wideband oscilloscope these peaks can be as high as the individual arc discharges which are discussed next. The main point here is that the steady-state e^3 condition is best described as being corona-like and is very noisy. One other important aspect of enhanced electron emission is its very localized nature. By covering successively smaller halves of the test sample surface with 5 mil Kapton, nearly the entire emisson current was found to be emitted from less than 1/128 of the total sample area. This small exposed area, of course, included some metal and some dielectric. Thus, e^3 currents are emitted from a extremely localized source, and should not be considered as a per unit area phenomenon such as the charging process.

Arc discharges due to negative metal-positive dielectric charges were investigated at the diagnostic points shown in Figure 6 using a wideband oscilloscope and Polaroid camera. Most of the oscilloscope waveform records were taken with C_1 equal to 100 pf (a 1 meter radius spacecraft), and C_2 equal to .05 μf, a 500:1 voltage division ratio. Figure 10a is the substrate voltage waveform showing a rise from the predischarge potential (-3 kV) to

zero volts in about 1.2 μs. The voltage falls back to the predischarge level in about 5 μs, a time defined by the spacecraft capacitance and the chargeup current defined by the series resistor, R_1, in our test setup. Figure 10b is the rate-of-change of current as measured by the loop antenna. Figure 10c is the substrate voltage when C_1 is made to be 0.1 μf and C_2 is replaced with a 50 ohm resistor. The voltage risetime is 6 μs, and the total pulsewidth is about 20 μs. Figure 10d is the voltage waveform at the first grid or mesh in front of the test sample, with C_1 equal to 100 pf. The mesh is collecting blowoff electrons most of the time except for a positive pip at the end due to ions. Figure 10e is the same mesh current when C_1 is 25 pf. The collected current is ionic for most of the time except for a short electronic pip at the beginning. For values of C_1 greater than 100 pf, the waveform is always negative. Figure 10f is the waveform at the second grid when it is biased negatively. Positive ions are collected after the first microsecond with a risetime of about 6 μs. The ionic current pulse lasts for about 6 ms. These waveforms demonstrate that the discharges are not purely electronic, but that ions are intimately involved in the discharge process.

DISCUSSION AND CONCLUSIONS

The test results reported here characterizing the EMI generated by negative metal/positive dielectric voltage stresses are not all-encompassing nor complete. However, important data has been obtained:

- Enchanced electron emission I-V curves
- e^3 corona noise vs e^3 steady-state current
- Localized nature of e^3 and negative metal arc discharge currents
- Negative metal arc discharges at stress thresholds below 1 kilovolt
- Negative metal arc discharge characteristics
- Dependence of blowoff arc discharge current on spacecraft capacitance to space (linear dimension)
- Damage to second surface mirrors due to negative metal arcs

Among the arc discharge parameters of interest are the relatively slow risetimes on the order of 1 μs for approximately 200 cm^2 sample sizes. A quick-look analysis of the phenomenology of a negative metal discharge as compared to that of a brushfire model developed for the opposite stress polarity, positive metal/negative dielectric, leads to many dissimilarities in the physical situations. For example, field emission of electrons is possible from a negative metal but not from a positive metal. The empirical data shows that risetimes are too slow for purely electronic processes, and the detection of an ionic component in the blowoff current indicates that many aspects of the brushfire model may yet be applicable. The slow risetime as compared to

discharges of the opposite polarity may have to do with the reduced breakdown voltage threshold rather than any fundamental difference in the on-going physical processes.

A significant aspect of the blowoff current is that it increases in magnitude as the spacecraft capacitance to space, C_1 in our test, increases. Figure 11 shows the linear rise of peak discharge current vs C_1 obtained in our tests. Our test data also indicate that, unlike the prediction of the brushfire theory for discharges of the opposite polarity, the blowoff current source is localized rather than moving over the surface at the head of the brushfire wavefront. The cracking of second surface mirrors, not observed with the positive metal polarity, is a further indication of this aspect of negative metal discharges.

Much more work needs to be done in understanding the phenomenology of negative metal/positive dielectrics discharges, and in characterizing the various associated EMI parameters. For example, the dependence of discharge characteristics on sample area, sample thickness and sample material have not been determined, and a basic phenomenological model has not been developed which is completely consistent with our physical intuition and the observational data. The authors acknowledge the skillful assistance of J. R. Valles in obtaining the laboratory test data.

REFERENCES

1. G. T. Inouye and M. J. Sellen Jr., "TDRSS Solar Array Arc Discharge Tests", Spacecraft Charging Technology-1978, NASA CP-2071, AFGL-TR-79-0082, 1979.

2. N. J. Stevens, H. E. Mills and L. Orange, "Voltage Gradients in Solar Array Cavities as Possible Breakdown Sites in Spacecraft-Charging-Induced Discharges", IEEE Transactions on Nuclear Science, Volume NS-28, No. 6, December 1981.

3. G. T. Inouye and R. C. Chaky, "Enhanced Electron Emission from Positive Dielectric/Negative Metal Configurations on Spacecraft", IEEE Transactions on Nuclear Science, Volume NS-29, No. 6, December 1982.

4. H. C. Koons, "Summary of Environmentally Induced Electrical Discharges on the P78-2 (SCATHA) Satellite", AIAA 20th Aerospace Sciences Meeting, January 1982.

5. G. T. Inouye, "Brushfire Arc Discharge Model", Spacecraft Charging Technology-1980, NASA CP 2182, AFGL-TR-81-0270.

TABLE 1. - CHARACTERISTICS OF INDIVIDUAL SOLAR CELL SAMPLES. (Samples 1, 2, 9, and 10 are most nearly flight-like.)

SAMPLE NUMBER	COVER GLASS MATERIAL	INTERCONNECTS USED	KAPTON USED AS INSULATION
1	FUSED SILICA	STANDARD	YES
2	CERIA GLASS	STANDARD	YES
3	FUSED SILICA	IN-PLANE	YES
4	CERIA GLASS	IN-PLANE	YES
5	FUSED SILICA	NONE	YES
6	CERIA GLASS	NONE	YES
7	FUSED SILICA	NONE	NO
8	CERIA GLASS	NONE	NO
9	FUSED SILICA	STANDARD	YES
10	CERIA GLASS	STANDARD	YES

TABLE 2. - SOLAR CELL TEST SUMMARY

SAMPLE NUMBER	PHOTOEMISSION CURRENT (NA)	ARCING	ENHANCED ELECTRON EMISSION
1	4.0	YES	YES
2	4.1	YES	NO*
3	4.0	YES	NO
4	3.4	YES	NO
5	0.7	YES	NO
6	0.042	YES	NO
7	29.0	YES	YES
8	20.6	YES	NO*
9	3.6	YES	NO*
10	5.5	NO	NO*

*WE HAVE OBSERVED E^3 PREVIOUSLY FOR THIS CONFIGURATION, BUT NOT THIS SAMPLE

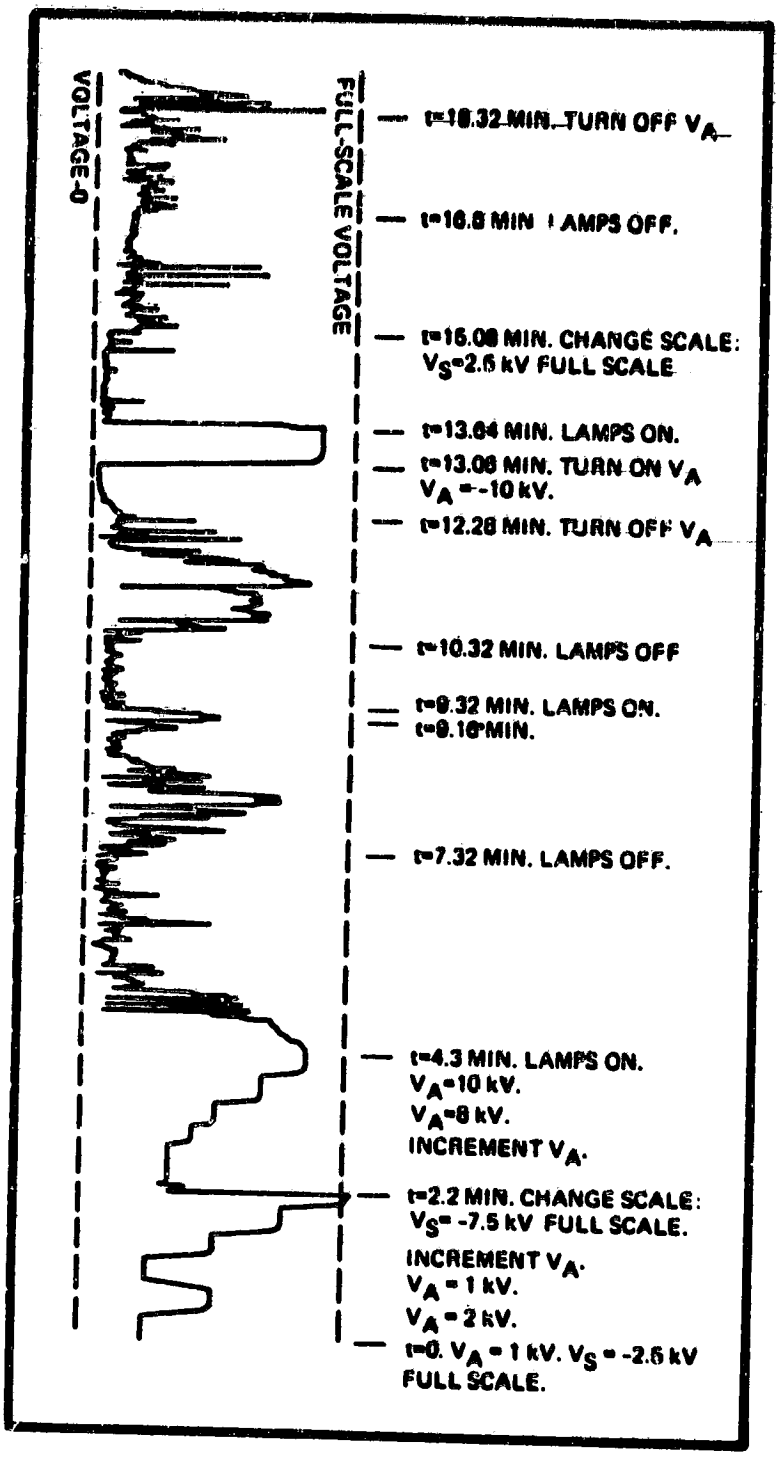

Figure 1. - Strip chart record of voltage variation in time, for solar cell sample. (This illustrates noisy voltage characteristic of enhanced electron emission.)

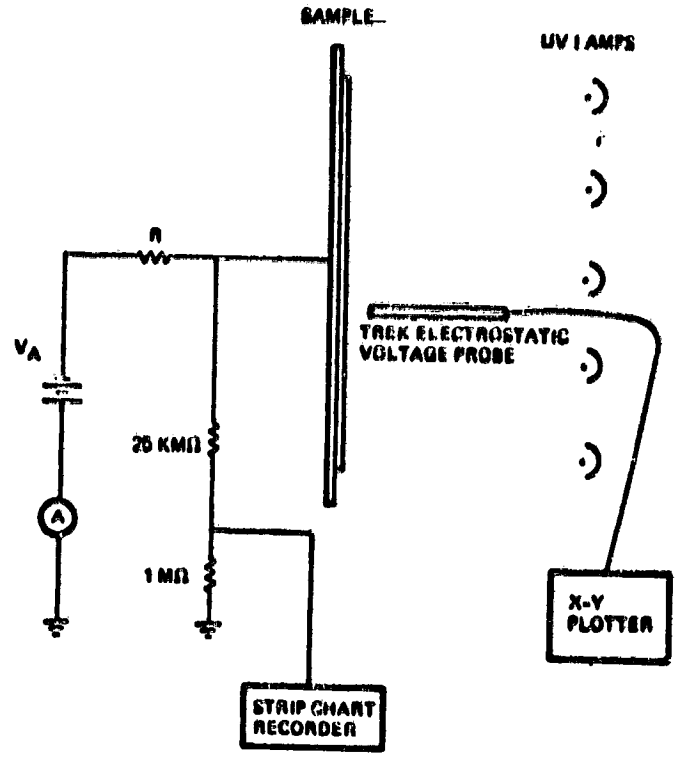

Figure 2. - Schematic of test setup using negative applied voltage and UV lamps.

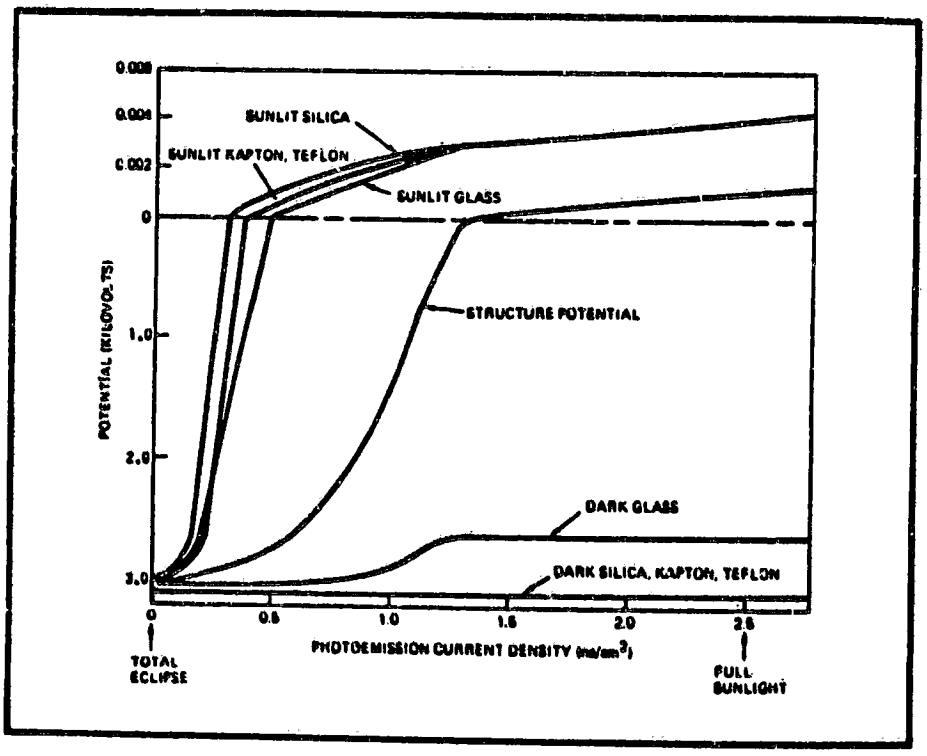

Figure 3. - Spacecraft surface potentials for NASA severe environment as function of photoemission current density, computed using TSCAT (TRW spacecraft charging technique).

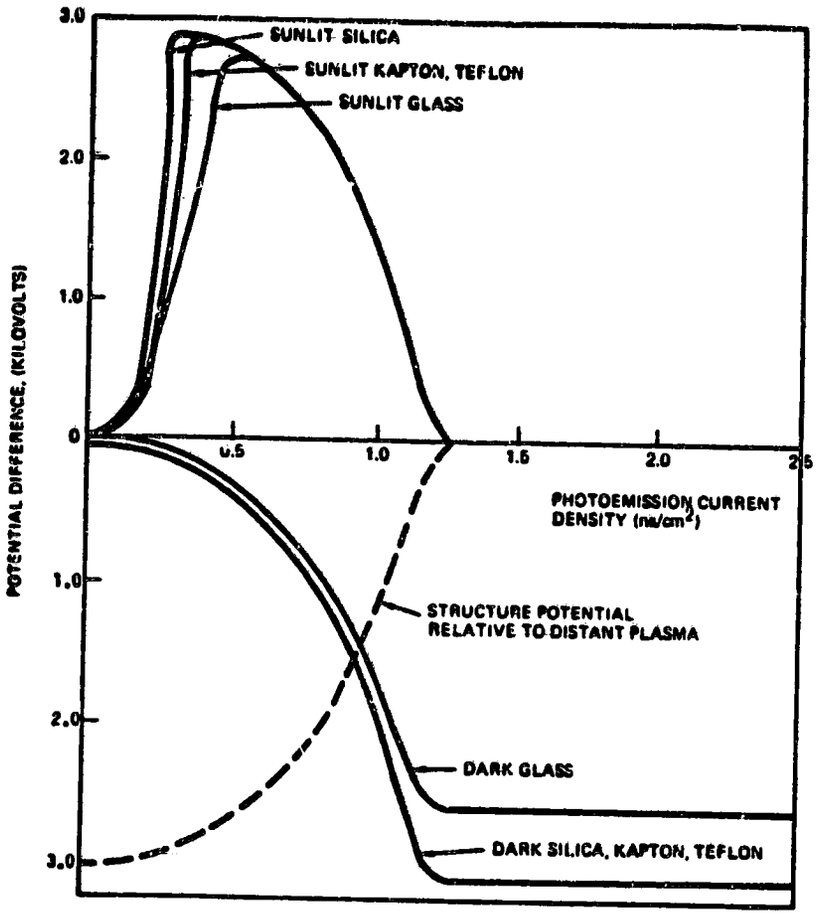

Figure 4. - Differential surface voltages corresponding to figure 3.

ORIGINAL PAGE IS
OF POOR QUALITY

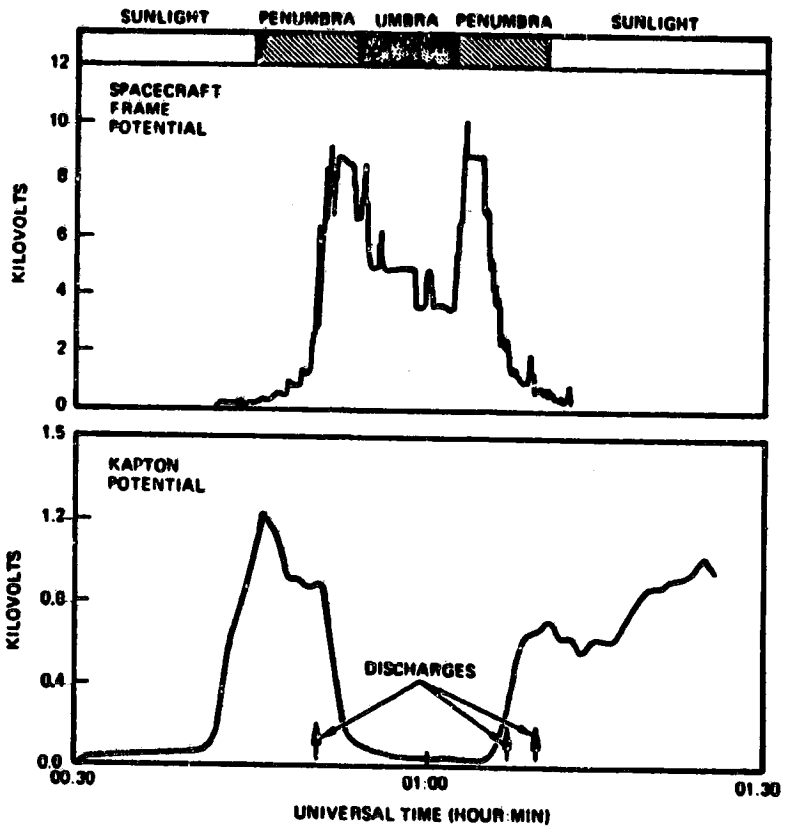

Figure 5. - Correlation of occurrence of arc discharges in SCATHA P78-2 spacecraft with reduced sunlight intensity with entrance and exit for eclipse (Coincides with peak in differential surface voltages from figure 4.).

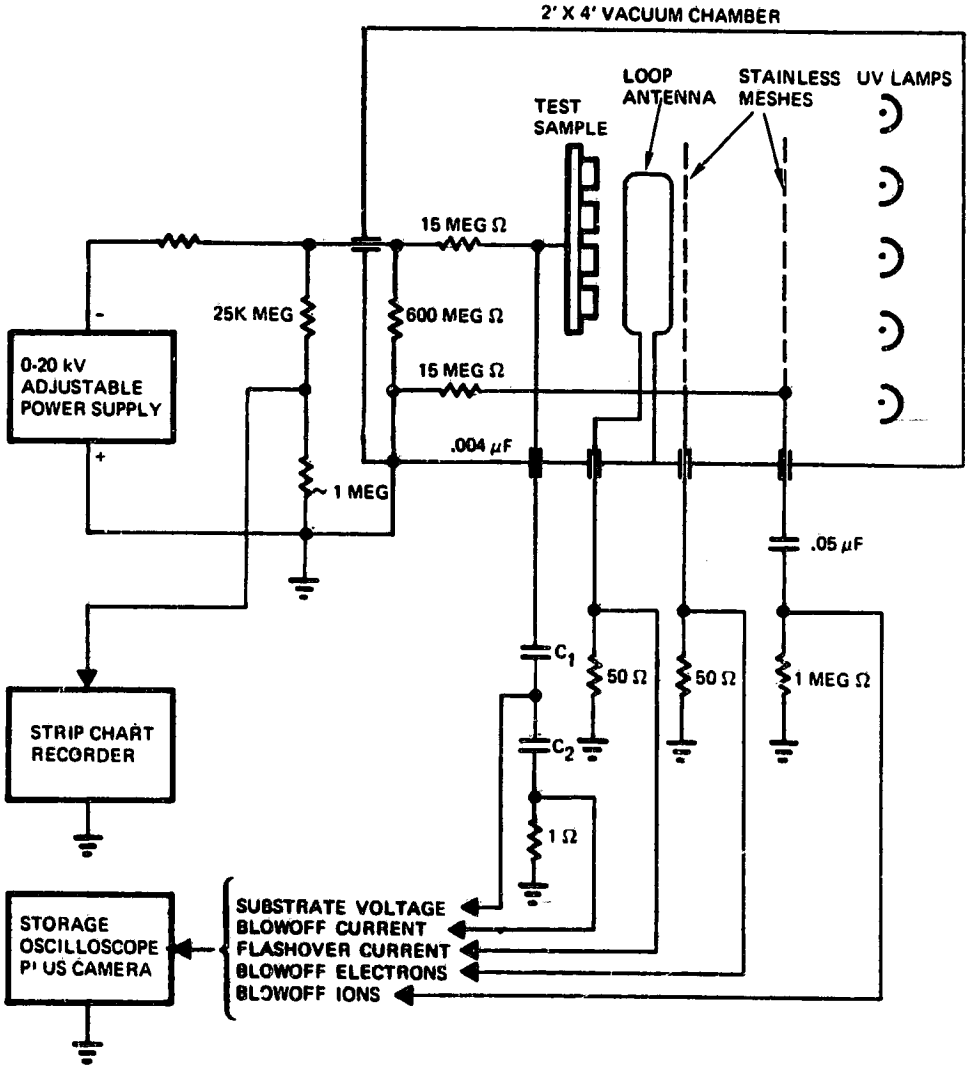

Figure 6. - Test setup to characterize negative metal EMI characteristics.

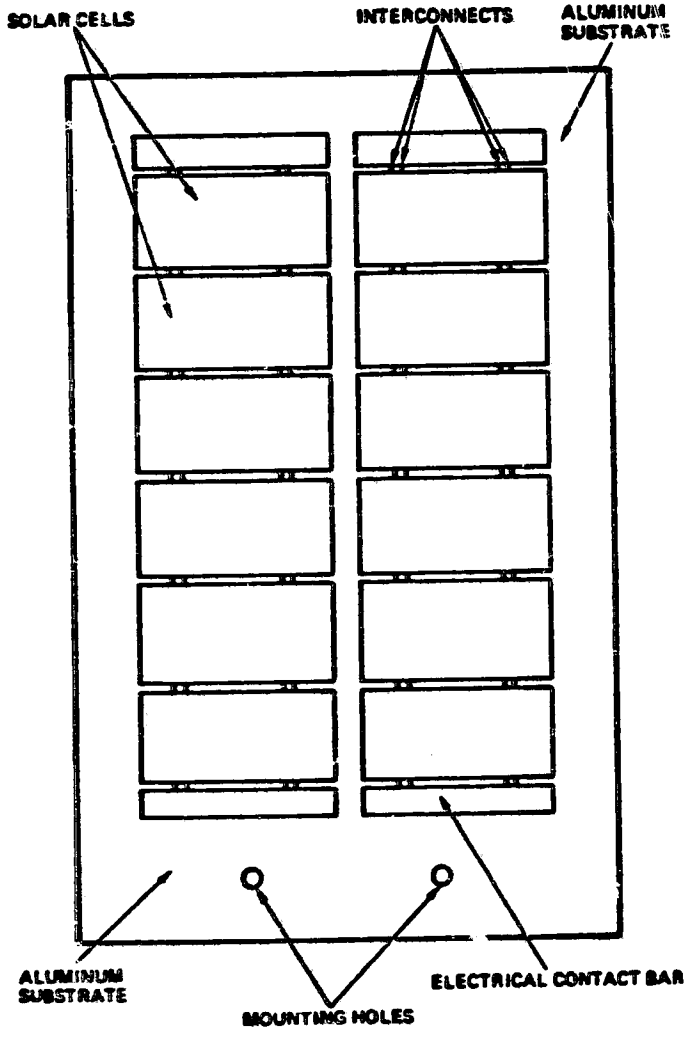

Figure 7. - Solar cell sample configuration.

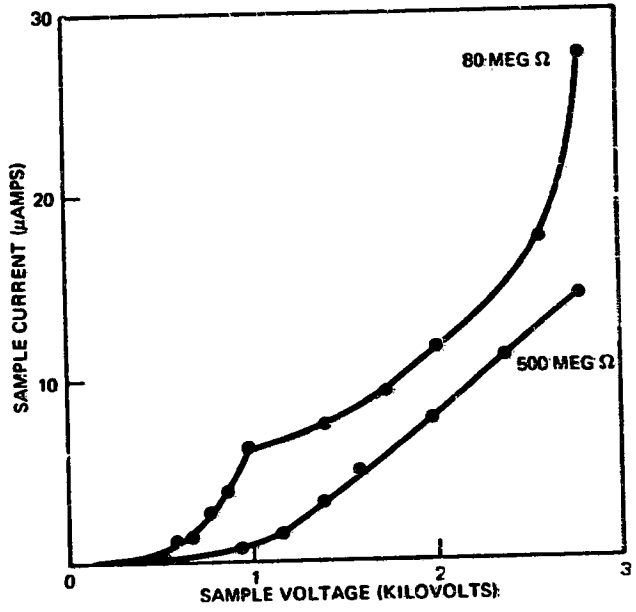

Figure 8. - Steady-state enhanced electron emission current versus sample voltage.

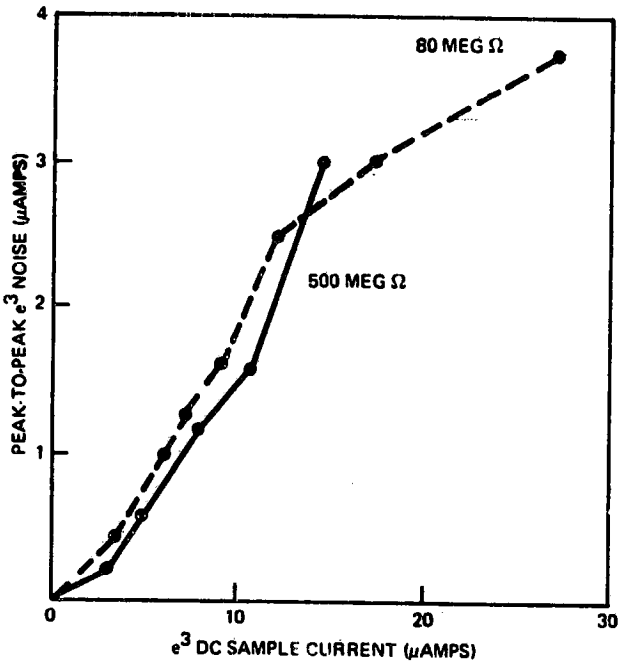

Figure 9. - Peak-to-peak enhanced electron emission (e^3) noise current versus dc e^3 current. (0-10 Hz).

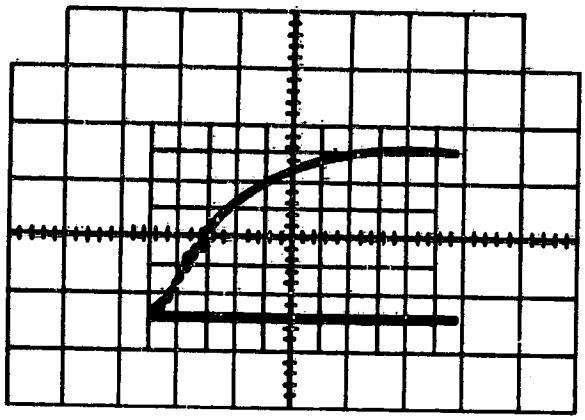

(a) Substrate voltage: C_1 = 100 pF; voltage from -3 kV to ground in 0.8 μsec.

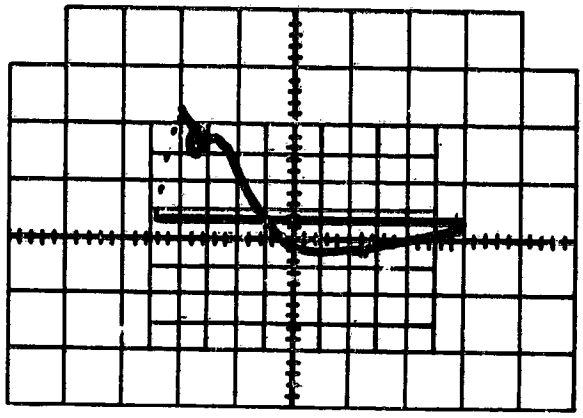

(b) Substrate replacement current: C_1 = 100 pF; peak = 0.5 A; rise-time = 0.4 μsec; width = 1.5 μsec.

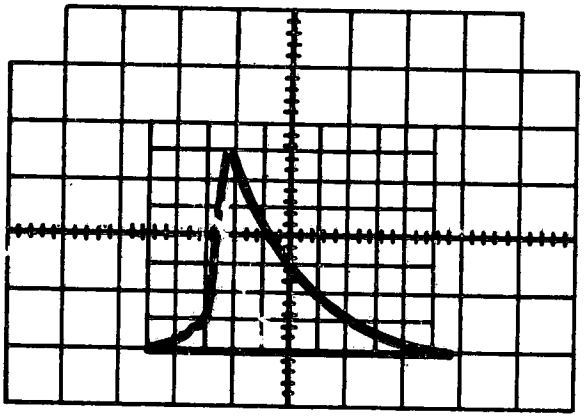

(c) Substrate voltage: C_1 = 0.1 μF; R = 50 Ω; risetime = 6 μsec; width = 20 μsec.

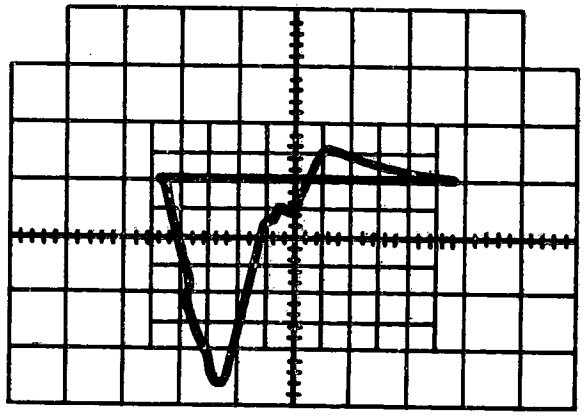

(d) First grid blowoff current: C = 100 pF; 1 μsec to negative peak (electrons).

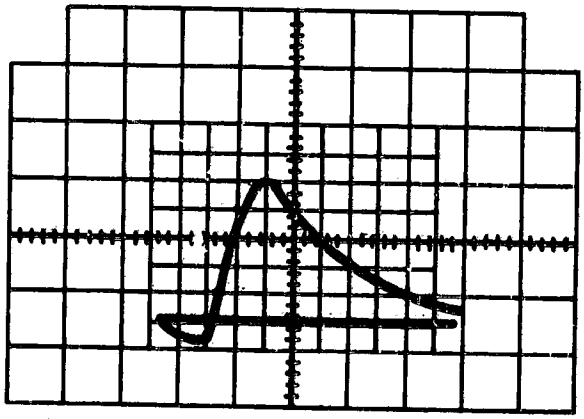

(e) First grid blowoff current: C_1 = 25 pF; 1 μsec to positive peak (ions).

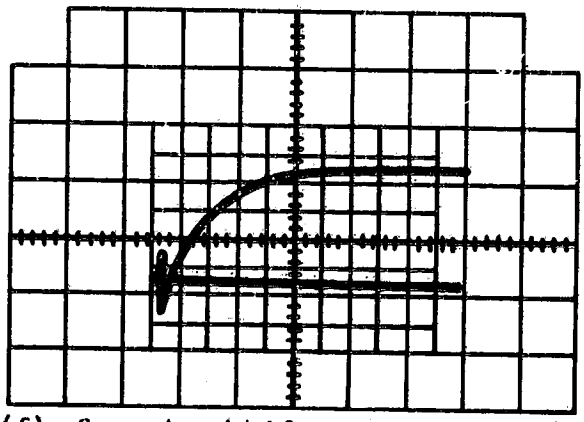

(f) Second grid blowoff current: Shows ion collection; risetime = 6 μsec.

Figure 10. - Negative metal arc discharge waveforms.

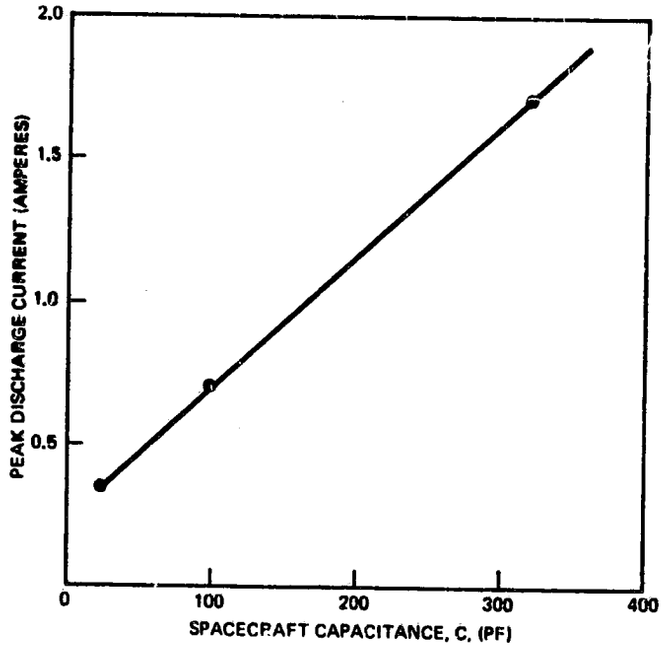

Figure 11. - Peak discharge current versus spacecraft capacitance.